Materials & Design 217 (2022) 110621

Contents lists available at ScienceDirect

Materials & Design

journal homepage: www.elsevier.com/locate/matdes

The effect of near-infrared light-assisted photothermal therapy combined with polymer materials on promoting bone regeneration: A systematic review

Siyi Wang [a,b], Feilong Wang [a,b], Xiao Zhao [a,b], Fan Yang [a,b], Yuqian Xu [a,b], Fanyu Yan [a,b], Dandan Xia [b,c,*], Yunsong Liu [a,b,*]

[a] Department of Prosthodontics, Peking University School and Hospital of Stomatology, Beijing 100081, China
[b] National Center of Stomatology, National Clinical Research Center for Oral Diseases, National Engineering Research Center of Oral Biomaterials and Digital Medical Devices, Beijing Key Laboratory of Digital Stomatology, Research Center of Engineering and Technology for Computerized Dentistry Ministry of Health, NMPA Key Laboratory for Dental Materials, Beijing 100081, China
[c] Department of Dental Materials, Peking University School and Hospital of Stomatology, Beijing 100081, China

HIGHLIGHTS

- Near-infrared light-assisted photothermal therapy and polymer scaffolds can synergistically enhance bone regeneration.
- Polymer scaffolds are used as the delivery vehicles for photothermal agents and tissue supports in bone tissue engineering.
- Polymer scaffolds could be made into various forms, such as coatings, 3D scaffolds, membranes and injectable hydrogels.
- The hyperthermia has a good effect on bone defect repair, anti-tumour, antibacteria and osseointegration of implants.
- Combined with photothermal therapy, the polymers obtain a higher spatiotemporal precision in promoting bone regeneration.

GRAPHICAL ABSTRACT

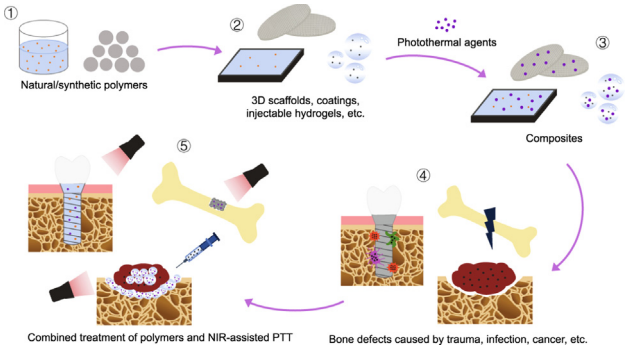

ARTICLE INFO

Article history:
Received 18 November 2021
Revised 17 March 2022
Accepted 3 April 2022
Available online 5 April 2022

Keywords:
Near-infrared light
Photothermal therapy
Bone tissue engineering
Polymers
Bone regeneration

ABSTRACT

Bone tissue engineering (BTE) has become a promising method for treating bone defects in recent decades. Polymers are effective materials currently used in the field of BTE due to their diverse characteristics and easy processing performance, which are categorised into natural polymers and synthetic polymers. Photothermal effects produced by near-infrared (NIR) light constitute an effective way to promote osteogenesis, with the advantages of being non-invasive and having high spatial and temporal precision. The main objective of this systematic review was to reveal the current applications of NIR light-assisted photothermal therapy (PTT) with polymer scaffolds as the delivery vehicles for photothermal agents and tissue supports in BTE. The databases collection was completed on October 1, 2021, and a total of 21 relevant studies were finally included. According to the retrieved literatures, we outlined that polymers could be made into various forms, such as coatings, three-dimensional (3D) porous scaffolds, membranes and injectable hydrogels, etc., and that the hyperthermia generated by PTT has a good effect on

* Corresponding authors at: Peking University School and Hospital of Stomatology, No.22, Zhongguancun South Avenue, Haidian District, Beijing, 100081, China.
E-mail addresses: dandanxia@pku.edu.cn (D. Xia), liuyunsong@hsc.pku.edu.cn (Y. Liu).

https://doi.org/10.1016/j.matdes.2022.110621

osteogenesis, as well as anti-tumour, antibacterial and osseointegration around the implants. These findings have revealed that the joint application of BTE polymer scaffolds and NIR light-assisted PTT play a positive role in bone regeneration.

Contents

1. Introduction

Bone defects caused by trauma, infection, cancer and so on are common clinical problems that can cause continuous suffering to patients and pressure on the healthcare system [1,2]. For the treatment of bone defects, autografts are considered to be the "gold standard", however, they have disadvantages such as limited available sources, pain at the donor sites, immune response and potential risk of infection [3–5]. Recently, bone tissue engineering (BTE) has been used as a promising candidate for constructing bone graft substitutes aimed at overcoming these shortcomings. BTE scaffolds loaded with cells and growth factors are expected to mimic the structure and composition of natural bone extracellular matrix, and by implanted into the body, they help repair the defective bone tissues [6,7]. In recent decades, with the rapid development of three-dimensional (3D) printing technology, the composition and structural design of scaffolds have been continuously innovated to achieve better osteogenic properties [8,9].

To develop precise treatment methods to maximise the effectiveness of osteogenesis and bone regeneration, and minimise the adverse effects on surrounding healthy tissues, hyperthermia is considered to be an ideal method to enhance the treatment of bone defects [10–12]. It has been proposed that the temperature of hyperthermia beneficial to bone regeneration is 40–42 °C [13]. A commonly used hyperthermia strategy is photothermal therapy (PTT), which directly uses photothermal agents (PTAs) to convert the light energy of near infrared (NIR) light into thermal effects [10,14]. NIR light-assisted PTT has the advantages of high efficiency, non-invasiveness, and high spatiotemporal accuracy [15]. NIR light with a wavelength range of 700–1300 nm is usually used because of its extended penetration depth into biological tissues, which could trigger biological events non-invasively and has few side effects [12,15]. Moreover, as PTAs are placed in local tissues to convert light energy into heat energy and transmit it to nearby cells, PTAs with ideal photothermal conversion efficiency is a key factor of PTT. Thus far, many PTAs such as gold nanostructures, copper-based nanomaterials, black phosphorus and red phosphorus, and carbon-based nanomaterials such as graphene oxide have been widely used [16–19].

For the PTAs to enter the body, a delivery vehicle is necessary. The BTE scaffolds can be used as templates to allow the growth of tissues, provide structural support, and serve as carrier for PTAs, cells, and drugs [20,21]. Therefore, BTE scaffolds combined with PTAs at the defect sites could produce a photothermal response to external NIR light and, thus, accelerate the bone healing process. So far, different types of biomaterials such as ceramics, metals, natural and synthetic polymers, or their composite materials have been made into scaffolds to mimic the behaviour of natural bones to a certain extent [22–25].

Polymers are extensively used in BTE due to their diverse characteristics and easy processing performance. According to the origin, polymers are divided into natural ones and synthetic ones [26]. Natural polymers can be found in natural tissues, and they have the advantages of biodegradability, ideal cellular responses and biological properties [27]. On the other hand, synthetic polymers are artificially synthesised, and can thus be stably produced on a large scale, with adjustable physical, chemical and mechanical properties [28].

To illustrate the effect of the combined application of BTE polymer scaffolds and PTT in the treatment of bone defects, this article systematically reviewed the latest developments in the use of NIR light-assisted PTT for bone regeneration, with polymers used as delivery vehicles and biomimetic support structures. This systematic overview will help in the precise therapeutic design of composite materials used in the treatment of bone-related diseases.

2. Methods

PubMed, Embase, and Web of Science databases were searched for articles published up to October 1, 2021. Keywords were used

as follows: (((NIR) OR (Near infrared)) AND (((((Bone regeneration) OR (Osteogenesis)) OR (Bone Formation)) OR (Ossification)) OR (Osteoconduction))) AND (polymer). A total of 102 relevant studies were revealed according to the keywords, and they were further screened based on the following inclusion and exclusion criteria.

Inclusion criteria: (1) PTT is used for bone regeneration, including simple bone defect repair, tumour-related bone defect treatment, osseointegration on implant surfaces, bone infection treatment, etc.; (2) Polymers are used as carriers of PTAs and support materials, including natural polymers, synthetic polymers, or their composites; (3) Polymers are used in different forms, such as scaffolds or coatings, etc.; (4) NIR light is used to generate photothermal effect.

Exclusion criteria: (1) Duplicate studies; (2) Studies without using NIR light or PTT; (3) Studies without using polymers; (4) Articles in languages other than English.

All the retrieved articles were first selected based on titles and abstracts, articles that did not match the topic were excluded. Potentially suitable articles were then assessed according to the inclusion and exclusion criteria. For further detailed screening, the full texts of remaining articles were evaluated. Finally, a total of 21 articles fulfilled the eligibility criteria were screened out and fully discussed, the selection process was shown in Fig. 1. The publication year and keywords of each study were summarised in Fig. 2 and Fig. 3. In the Fig. 3, the closer to the centre, the more times the keyword was mentioned, and vice versa.

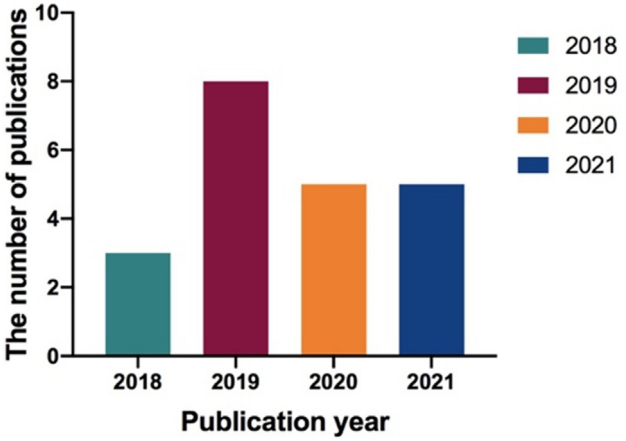

Fig. 2. Publication years of included articles.

3. Results

3.1. Polymers used in selected articles

Among the 21 included studies: five used natural polymers: [29,30,31,32,33]; nine used synthetic polymers: [13,34,35,36,37,38,39,40,41]; and seven used composites thereof: [42,43,44,45,46,47,48] (Fig. 4). Among them, the most used natural polymer was chitosan, and alginate and gelatine were also used. The most used synthetic polymer was PDA, besides, PLGA, PLA, PCL, PEG, PVA and PEEK were also used. Polymers were mainly made into coatings, 3D porous scaffolds, membranes, microspheres, and injectable hydrogels to promote bone regeneration. Since bone metastasis of tumour can cause bone defects, and bacterial contamination on the surface of implants will affect the osseointegration, the elimination of tumours and bacteria will also promote the healthy growth of bone tissue. Thus, from the included articles, it could be found that functions like anti-tumour and anti-bacterial properties generated by PTT were usually studied altogether. Moreover, it is worth noting that there were four studies that fabricated drug-delivering systems that improved the therapeutic effect [29,42,44,46]. The commonly used experimental models for *in vivo* studies could be roughly divided into four categories: cranial defect, femoral/tibia defect, dorsal/flank/armpit subcutaneous implantation or tumour, and alveolar bone defect. The specific

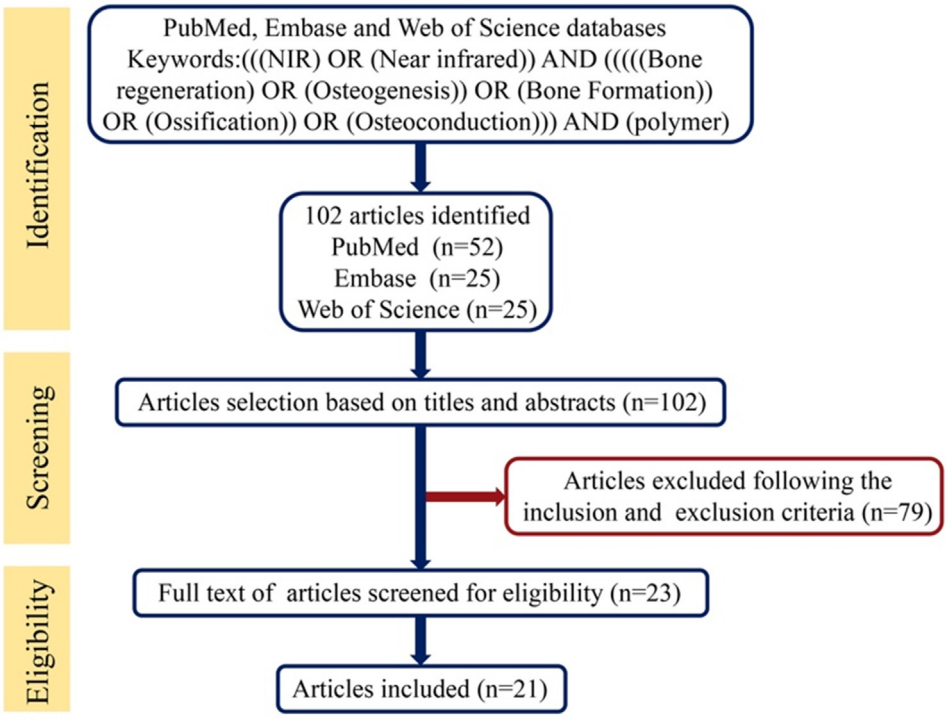

Fig. 1. Flow chart of the selection process.

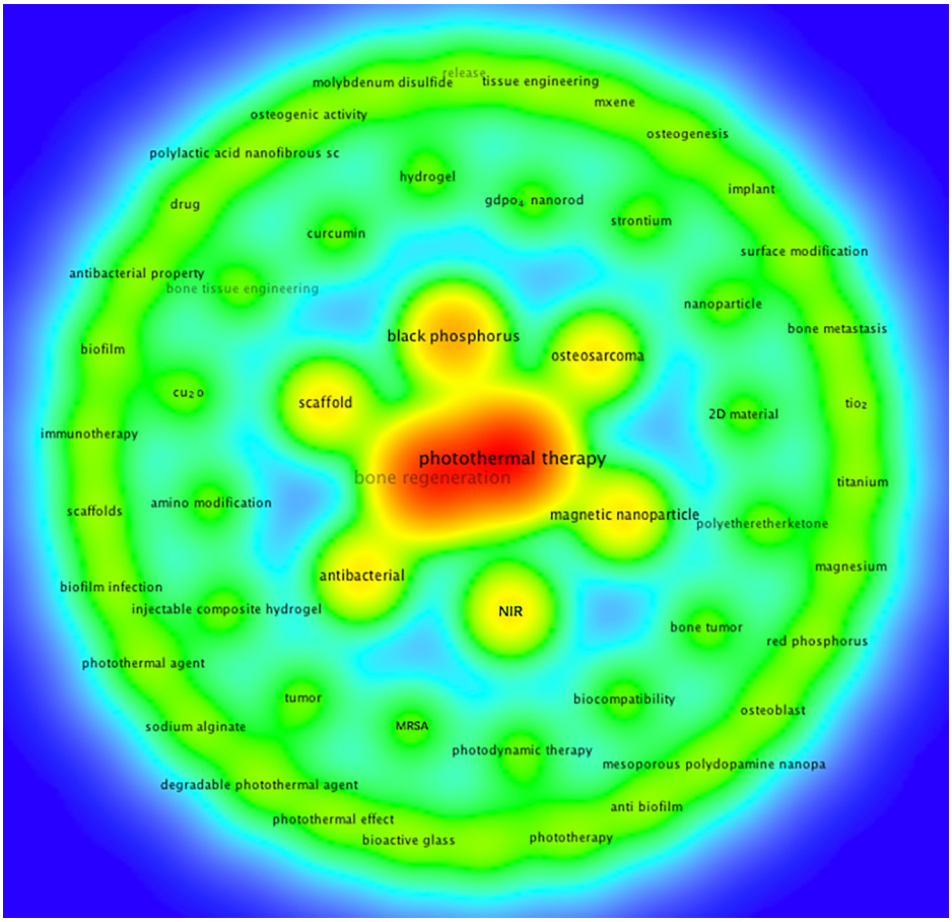

Fig. 3. The summary of keywords from each included studies.

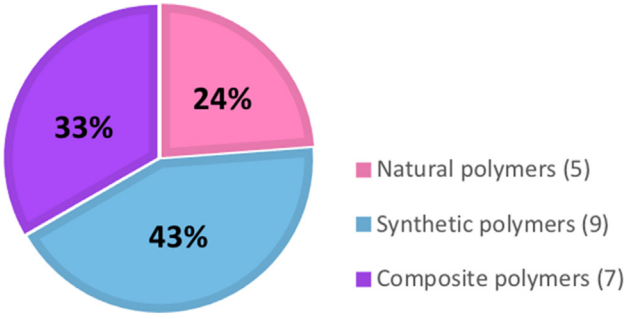

Fig. 4. The number and proportion of included articles using natural polymers, synthetic polymers, and composites thereof.

application fields, material forms and *in vivo* research methods were summarised in Fig. 5.

3.2. NIR photothermal agent and light radiation conditions

Among the 21 included studies: six studies used metal oxide particles as the photothermal agent; one study used metal particles; five studies used carbon-based materials; five studies used black or red phosphorus; and four studies directly used the synthetic polymer PDA. As for the NIR light wavelength, 19 studies used 880 nm, one study used 1064 nm [40], and one study did not specify the wavelength [45]. To collect more comprehensive information of the radiation conditions, we obtained more detailed parameters such as the power density and radiation time of the NIR light, and the mechanisms of their effect on osteogenesis. All the critical information of the included studies were listed in Table 1, Table 2, and Table 3, classified by natural polymers, synthetic polymers and composite polymers, respectively.

3.3. The evaluation of keywords from the included literatures

In Fig. 3, the closer the keywords are to the centre of the circle, the more times they were mentioned in the included articles. It could be seen that in addition to the two core keywords "photothermal therapy" and "bone regeneration", the other two keywords "osteosarcoma" and "antibacterial" appeared very frequently in the included literatures. This suggests that PTT may be frequently used to treat bone defects associated with tumours and infections. In addition, it could be seen that compared with 2D materials and coatings, three-dimensional scaffolds are currently a relatively hot application form in bone defect repair, as "scaffold" was frequently mentioned. Finally, at the level of PTAs, the most frequently occurring keywords were "black phosphorus" and "magnetic nanoparticle", indicating that these two materials are stable, easy to obtain and efficient in exerting photothermal effects.

3.4. The practical stages of included studies

Among the 21 included articles, 18 studies were conducted at the animal experiment level, 8 of which used two animal models: [29,30,33,35,40,41,42,48], and 10 used one animal model: [13,31,34,36,37,38,39,43,44,45]. The animal models used were cal-

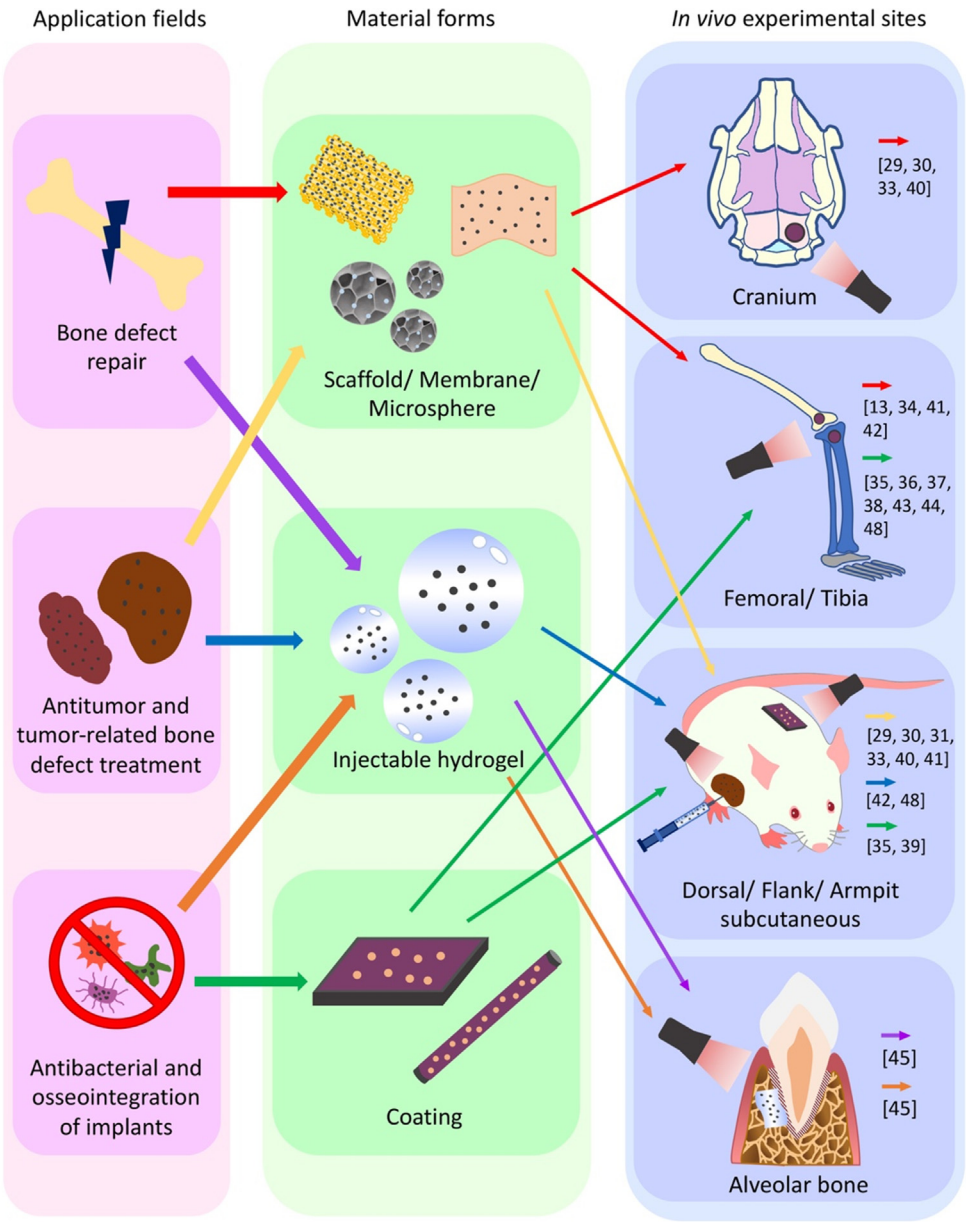

Fig. 5. The application fields, material forms and *in vivo* experimental sites summarised from the included articles. Different coloured arrows indicated different applications. Red arrow: Scaffolds, membranes or Microspheres used for bone defect repair. Purple arrow: Injectable hydrogels used for bone defect repair. Yellow arrow: Scaffolds, membranes or microspheres used for antitumour and tumour-related bone defect treatment. Blue arrow: Injectable hydrogels used for antitumour and tumour-related bone defect treatment. Orange arrow: Injectable hydrogels used for antibacterial and osseointegration of implants. Green arrow: Coatings used for antibacterial and osseointegration of implants.

varia defects of rats: [29,30,33,40]; femoral/tibia defects of rats: [13,34,35,36,37,38,41,43,44,48]; femoral/tibia defects of rabbits: [42]; alveolar bone defects of rats: [45]; subcutaneous of rats/mice: [29,30,31,33,35,39,40,41,42,48]. In addition, there were 3 studies only performed *in vitro* experiments: [32,46,47]. It is worth noting that none of the studies have entered the stage of clinical trials.

4. Discussion

According to the number and publication years of the included articles, it could be seen that the combined application of NIR light-assisted PTT and polymer materials in bone defect treatment has not been extensively studied. Therefore, in-depth research in this field can be carried out to provide new options for the development of novel therapies for bone regeneration. The insights brought by this systematic review are discussed below.

4.1. The application of NIR light-assisted PTT

Hyperthermia therapy has been widely used for many bone-related diseases. It has been observed that hyperthermia (42.5–44 °C) of rabbit femurs after initial surgical trauma stimulated bone remodelling, formation of new bone trabeculae, and increased cortical bone density [49]. In addition, Shui et al. observed that the expression level of alkaline phosphatase (ALP) of bone marrow mesenchymal stem cells (BMSCs) increased after a single exposure at 42.5 °C, and transient exposures to 39–41 °C greatly enhanced the mineralised nodules formation of BMSCs [50]. Tong et al. proposed that the temperature of hyperthermia

Table 1
Studies using natural polymers as tissue support and PTA carriers.

Material composition	Photothermal agents	Polymers and functions	Wavelength	Power density	Radiation time	Highest tissue temp.	Effects	Functional agents	Mechanisms	Reference
$SrFe_{12}O_{19}$- $CaSiO_3$-CS-DOX scaffold	M-type ferrite particles: $SrFe_{12}O_{19}$	CS, promote osteoblastic cells adhesion and differentiation and bone formation	808 nm	0.3 W/cm^2	6 min	44 °C	Enhance bone regeneration and photothermal-chemotherapy of osteosarcoma	DOX for anti-tumour efficacy; biopolymer CS promoted osteoblastic cells adhesion and differentiation and bone formation in vivo	Excellent anti-tumour efficacy was achieved via the synergetic effect of DOX drug release and hyperthermia ablation; BMP-2/Smad/Runx2 pathway was involved in the scaffolds promoted proliferation and osteogenic differentiation of hBMSCs	[29]
$SrFe_{12}O_{19}$- BG-CS scaffold	magnetic $SrFe_{12}O_{19}$ nanoparticles	CS, good biocompatibility, excellent osteoconductivity and appropriate biodegradability	808 nm	0.3 W/cm^2	6 min	43 °C	Enhance bone regeneration and photothermal therapy against tumours	Ca element from the degradation of BG particles promoted the deposition of bone-like apatite, the released Si element improved the viability and osteogenic differentiation of stem cells; CS was fit for osteoconductive matrix due to excellent biocompatibility	Under the irradiation of NIR, the elevated local temperatures of 42–50 °C promote tumour hyperthermia ablation; the expression levels of osteogenic-related genes and the new bone regeneration were promoted by the activation of BMP-2/Smad/Runx2 pathway	[30]
CD doped CS-nHA scaffold	Zero-dimensional CD	CS, has a rigid crystalline structure that promotes mesenchymal stem cells to differentiate into osteoblasts, and has notable biofunctions, including antimicrobial, antifungal, and antioxidant activities	808 nm	1.0 W/cm^2	10 min	51.4 °C	CD can enhance the osteogenesis-inducing property of bone repair scaffolds; CD doped scaffolds have potential for use in PTT for tumours and infections	CD synthesized from carbon nanopowder specifically bind to calcified bones in vivo; nHA is histocompatible and osteoinductive	Hyperthermia over 50 °C can damage DNA and cause irreversible protein denaturation in tumour cells; enhanced in vitro osteogenesis of rBMSCs by up-regulating their expression of osteogenic genes and significantly facilitated the formation of vascularized new bone tissue in vivo	[31]
Gel-Akr-Fe_3O_4-MWNT scaffold	MWNT, Fe_3O_4	Gelatine, biocompatible and biodegradable	808 nm	0.2, 0.6 and 1.0 W/cm^2	10 min	above 43 °C	Have a great potential in bone tissue engineering and probably treatment of tumour related bone defects	Gel and Akr provide adequate osteoinductivity, biodegradability, and mechanical properties	High temperatures above 43 °C can efficiently kill tumour cells through hyperthermia treatments; the scaffold possessed bone like apatite-formation ability and can release soluble ionic products to stimulate osteoblast proliferation	[32]
$GdPO_4$-CS-Fe_3O_4 scaffold	Fe_3O_4	CS, a typical natural material that provides a friendly microenvironment for cell attachment and extracellular matrix production	808 nm	4.6 W/cm^2	3 min	45.4 °C	Enable the photothermal ablation of postoperative residual tumours and subsequent bone defect healing	$GdPO_4$ nanorods served as a novel bioactive component for enhanced angiogenesis and osteogenesis abilities	Under the NIR laser irradiation, the local temperatures around the scaffolds were high enough to stimulate the apoptosis of tumour cells; the hydrated $GdPO_4$ nanorods in the scaffolds activated BMP-2/Smad/RUNX2 signalling pathway that facilitated cell proliferation, differentiation and bone tissue regeneration	[33]

CS = chitosan; DOX = doxorubicin; BG = bioglass; NIR = near-infrared; CD = carbon dots; nHA = nanohydroxyapatite; Gel = gelatine; Akr = akermanite; MWNT = multi-walled carbon nanotube.

Table 2
Studies using synthetic polymers as tissue support and PTA carriers.

Material composition	Photothermal agents	Polymers and functions	Wavelength	Power density	Radiation time	Highest tissue temp.	Effects	Functional agents	Mechanisms	Reference
BPs-PLGA membrane	BP	PLGA, a degradable biopolymer approved by FDA, which is commonly used in tissue engineering and produces innoxious end-products such as H_2O and CO_2	808 nm	1.0 W/cm^2	450 s	41.0 ± 1.0 °C	Boasting good biodegradability with harmless end-products and osteogenesis mediated by NIR irradiation, this BPs-PLGA osteoimplant has large clinical potential as scaffolds for inducing the osteogenesis	BPs are employed as photothermal agents due to the excellent NIR response, and can degrade naturally into the nontoxic PO_4^{3-} in physiological environment for serving as necessary bone ingredient	The specimen mediated by low intensity and periodic NIR irradiation can effectively up-regulate the expressions of heat shock proteins and finally promote osteogenesis *in vitro* and *in vivo*	[13]
BP-$SrCl_2$-PLGA microsphere	BP	PLGA, one of the most successful biodegradable and biocompatible polymers approved by the FDA for controlled drug delivery systems	808 nm	1.0 W/cm^2	10 min	Above 45 °C (about 50 °C)	NIR light-triggered drug delivery system for bone regeneration	Sr is associated with stimulation of osteoblast differentiation and bone formation as well as inhibition of osteoclast activity and bone resorption	Under NIR irradiation, the external PLGA shells of the microspheres are disrupted resulting in release of Sr^{2+} and $SrCl_2$; the release of Sr promotes bone regeneration	[34]
MoS_2-IR780-RGDC-PDA coating	MoS_2, a biocompatible prototypical transition-metal dichalcogenide that exhibits high photothermal conversion efficiency	PDA, attach the coating to the Ti implant surface	808 nm	0.5 W/cm^2	20 min	50 °C	By combing PTT and PDT, a photoresponsive system combining the function of biofilm eradication and osteogenic differentiation simultaneously was developed	IR780 is a photosensitizer that can transfer the energy of NIR light to $^3O_2$ to generate $^1O_2$; RGDC is natural bioactive material that can promote osteoconductivity	ROS could assist the PTT; the catalytic activity of GSH oxidation was accelerated by heat induced by NIR light irradiation, which explains the rapid bacterial death under hyperthermia; RGDC modification provided excellent osteoconductivity	[35]
RP-IR780-RGDC-PDA coating	RP	PDA, attach the coating to the Ti implant surface	808 nm	0.5 W/cm^2	10 min	50 °C	High effective antibacterial efficacy provided by PTT; the RGDC decorated surface possess an excellent performance in osteogenesis *in vivo*	With the effect of photothermal effect by RP and ROS produced by IR780, the biofilm could be eradicated; the osteogenic ability could be enhanced by RGDC	The IR780 functions to generate ROS which shows great synergistic action to kill bacteria with combination of PTT; the existence of RGDC makes it possible to accelerate the osteogenesis	[36]
MoS_2-PDA- RGD coating	MoS_2, display high photothermal conversion efficiency in the NIR region	PDA, incorporate RGD peptide onto MoS_2 nanosheets via PDA-assisting covalent immobilization	808 nm	1.0 W/cm^2	10 min	51.5 °C	Not only improved the osteogenesis of MSCs, but also endowed Ti substrates with effective antibacterial ability when exposing to NIR irradiation.	MoS_2 nanosheet, as one kind of graphene-like transition metal dichalcogenides, exhibits striking antibacterial property; RGD peptide was effective for improving osteogensis of bone-forming cells	Hyperthermia accelerated GSH oxidation and made bacteria more sensitive to oxidative stress;the cellular osteogenic behaviors was significantly increased via up-regulating osteogenesis-related genes (ALP, Runx2, Col I and OCN)	[37]
MPDA-ICG-RGD coating	MPDA	MPDA, an important bridge to fabricate biofunctional interface on an implant, exhibiting desirable adhesion	808 nm	2.0 W/cm^2	10 min	51.3 °C	Eradicate already-formed biofilm *in vivo* in a remotely controllable fashion and display effective osteogenesis and osseointegration	ROS generation from ICG induced the bacterial membrane destruction; RGD peptide facilitated cell adhesion, proliferation and differentiation and osseointegration *in vivo*	Osteogenic behaviors was significantly increased via up-regulating osteogenesis-related genes (ALP, Runx2, Col I and OCN)	[38]

(*continued on next page*)

Table 2 (*continued*)

Material composition	Photothermal agents	Polymers and functions	Wavelength	Power density	Radiation time	Highest tissue temp.	Effects	Functional agents	Mechanisms	Reference
TiO_2-MoS_2-PDA-RGD NAs coating	MoS_2, has high photothermal conversion efficiency in the NIR region	PDA, an excellent platform and stabilizer for the immobilization of a variety of organic and inorganic materials with special functions	808 nm	0.5 W/cm^2	10 min	50.2 °C	Effective antibacterial activity against S. aureus within 10 min as well as outstanding osteogenic properties	TiO_2 has good photocatalytic characteristics and can produce ROS; RGD improves cell adhesion, proliferation, and osteogenic differentiation	The synergistic effects of the generated hyperthermia and ROS increase the bacterial membrane permeability; nanostructure of TiO_2-MoS_2 NAs could promote the osteogenic activity; RGD promoted osteogenesis	[39]
$SrCuSi_4O_{10}$ nanosheets-PCL composite scaffold	$SrCuSi_4O_{10}$ nanosheets	PCL, has been widely developed as 3D printed scaffolds due to its outstanding biocompatibility and superior rheological/ viscoelastic properties	1064 nm	1.0 W/cm^2	5 min	53.4 °C	Multifunctional bone scaffolds based on therapeutic bioceramics for repairing tumour-induced bone defects	$SrCuSi_4O_{10}$ nanosheets possessed excellent photothermal conversion efficiency and high biocompatibility	Osteosarcoma could be ablated by the hyperthermia;the enhancement of vascularized bone regeneration owing to the controlled and sustained release of bioactive ions (Sr, Cu, and Si)	[40]
PLGA-Mg scaffold	micro-sized particles of Mg	PLGA, Make up for the drawbacks of pure Mg implants, such as too fast degradation rate, much hydrogen gas formation, difficult to manufacture Mg-based porous scaffolds	808 nm	1.0 W/cm^2	3 min	57 ± 6.73 °C	The scaffolds achieved complete suppression of tumour recurrence in the presence of near-infrared laser irradiation, as well as efficient bone defect repair *in vivo*	Mg, a promising bioactive material for bone regeneration, exhibits excellent osteogenic activity	Selectively destroy the osteosarcoma Saos-2 cells by optimizing the photothermal temperature at 45–55 °C to achieve controlled Saos-2 cell ablation; activation of the AKT and β-catenin pathways of osteoblast cells to promote osteogenesis	[41]

BP = black phosphorus; Sr = Strontium; PLGA = poly(lactic-co-glycolic acid); FDA = Food and Drug Administration; RGDC = arginine-glycine-aspartic acid-cysteine; PDA = polydopamine; Ti = titanium; PTT = photothermal therapy; PDT = photodynamic therapy; NIR = near-infrared; $^3O_2$ = dissolved oxygen; $^1O_2$ = singlet oxygen; ROS = reactive oxygen species; GSH = Glutathione; RP = red phosphorus; RGD = arginine-glycine-aspartic acid; MSCs = mesenchymal stem cells; MPDA = mesoporous polydopamine; ICG = Indocyanine Green; NAs = nanorod arrays; PCL = polycaprolactone.

Table 3
Studies using composite polymers as tissue support and PTA carriers.

Material composition	Photothermal agents	Polymers and functions	Wavelength	Power density	Radiation time	Highest tissue temp.	Effects	Functional agents	Mechanisms	Reference
OSA-CS-nHA-DDP-PDA hydrogel	PDA	PDA, exhibits intense absorption in the NIR region, and converts absorbed light into heat; OSA and CS, perfect biocompatibility, biodegradability, and similarity to bone matrix components	808 nm	2.0 W/cm^2	2 min	43 °C	Promote the adhesion and proliferation of bone mesenchymal stem cells *in vitro* and further induce bone regeneration *in vivo*.	DDP, an antitumour drug	Temperature at approximately 43 °C causes long-term cell inactivation; nHA is a major inorganic component in bone tissues and is composed of Ca and phosphorus elements that occupy active roles in bone formation; PDA adheres to cells and promotes cell proliferation.	[42]
NO plus $^{\bullet}O^{2-}$-RP-CS-PDA-PVA hydrogel coating	RP	PDA, excellent bonding performance and photothermal property; PVA, base material of the hydrogel; CS, utilized as the antibacterial component	808 nm	1.0 W/cm^2	20 min	45.1 °C	Biofilm was removed efficiently by synergetic photothermal bacteria killing and NO therapy as well as immunological therapy, and excellent bone formation was achieved	A low concentration of exogenous NO can enter bacteria and provide a degree of antimicrobial activity	Bacterial biofilms can be eliminated through pure PTT strategy at a high temperature; the released NO promoted osteogenesis activity; OPN and OCN were upregulated	[43]
SP-MXene-GelMA-PDA-TOB coating	MXene, $Ti_3C_2T_x$-based MXenes have a broad light absorption capacity from ultraviolet to NIR light and high photothermal conversion efficiency	SP, more similar to human cortical bone, reduce the risk of osteoporosis and osteonecrosis caused by stress shielding; GelMA, water-rich feature, excellent cytocompatibility, biodegradability, and nonimmunogenicity; PDA, a substrate-independent and flexible surface modification approach, also used as a photothermal material	808 nm	1.5 W/cm^2	10 min	49.1 °C	Not only defeat osteosarcoma cells and bacteria but also intensify osteogenicity	TOB is an antibacterial drug	GelMA hydrogels induce osteo-differentiation of stem cells and accelerate bone regeneration because they possess the inherent cell attachment-promoting RGD sequences; exposure to the ambient temperature above 48 °C can cause irreversible damage to the cancer cells	[44]
Cu_2O-TiO_2-PDA-SA hydrogel composite	PDA	PDA, has photothermal effect; SA hydrogel, could self-adapt to variform bone defects on account of its liquid-to-solid gelation process to match with variable morphologies accurately	––	1.0 W/cm^2	18 min	42 °C	Through dual-light (blue and NIR) noninvasive regulation, switch antibacterial and osteogenic modes to address requirements of patients at different healing stages	Cu_2O nanoparticles have high-efficiency, broad-spectrum, and long-term antibacterial effect; TiO_2-PDA could produce ROS under blue light (BL) irradiation to exhibit antibacterial performance	ROS could oxidize Cu^+ to Cu^{2+}, which combined with the NIR-mediated photothermal effect to promote osteogenesis; 42 °C is a proper temperature for osteogenesis	[45]

(*continued on next page*)

Table 3 (*continued*)

Material composition	Photothermal agents	Polymers and functions	Wavelength	Power density	Radiation time	Highest tissue temp.	Effects	Functional agents	Mechanisms	Reference
PLLA-BP-IBU-SA- Sr^{2+} nanofibrous scaffold	BP, display an excellent near-infrared photothermal-responsive drug release performance	PLLA nanofibrous, excellent degradability, biocompatibility and the biomimetic ECM topographies, improved hydrophilicity, osteoinductivity; SA, a natural polysaccharide, has excellent biocompatibility, environmental-friendliness, biodegradability and processability	808 nm	1.0 W/cm^2	5 min	42 °C	Improve cytocompatibility for cell proliferation and enhance osteogenic ability by promoting the formation of apatites	IBU is a non-steroidal antiinflammatory drug and is commonly used for pain relief, fever reduction and against inflammation; Sr^{2+} promote osteogenesis	The photothermal effect-induced hyperthermia can promote biomineralization by stimulating the up-regulated expression of proteins, including alkaline phosphatase ALP and HSP	[46]
CS-CM-PDA nanoparticles (CCPNPs)	PDA	CS, can be cross-linked with tripolyphosphate to form stable nanoparticles for the delivery of anticancer drugs; PDA, exhibited strong NIR light absorption properties and could induce photothermal conversion	808 nm	1.3 W/cm^2	10 min	–-	CCPNPs with bifunctional osteosarcoma therapy and bone repair may be an excellent candidate for local cancer therapy and bone regeneration	CM has anticancer activity and can enhance osteoblastic activity	The tumour cells were sensitive to the temperature range of 43–49 °C, which will accelerate their apoptosis; the activity of osteoblasts can be improved by adjusting the time or power of NIR radiation	[47]
SA-PEG-CuBGM injectable composite hydrogel	CuBGM	SA and PEG, the 3D network of composite hydrogel provides an extracellular matrix-like structure, fills the defect area, and provides a matrix for cell migration and proliferation	808 nm	0.75 W/cm^2 and 1.0 W/cm^2	10 min	56.4 °C	Available for photothermal therapy at the initial stage of implantation, and then the degradation of the photothermal agent and ion release can promote bone tissue repair	The photothermal effects were derived from the oxide formed by doping copper ions in CuBGM	The tumour cell membrane will collapse and protein denaturation will occur at temperatures above 50 ℃; Ca, Si and Cu released from CuBGM improved the osteogenic differentiation of mBMSCs by upregulating bone-related gene expression (ALP, Runx2, Col I and OPN)	[48]

OSA = oxidized sodium alginate; CS = chitosan; nHA = Nano-hydroxyapatite; DDP = cisplatin; DPA = polydopamine; RP = red phosphorus; NO = nitric oxide; $^{\bullet}O^{2-}$=superoxide; PVA = poly(vinyl alcohol); PTT = photothermal therapy; SP = sulfonated polyetheretherketone; GelMA = gelatine methacrylate; TOB = tobramycin; RGD = arginine-glycine-aspartic acid; SA = sodium alginate; ROS = reactive oxygen species; PLLA = poly-L-lactic acid; ECM = extracellular matrix; BP = black phosphorus; IBU = ibuprofen; ALP = alkaline phosphatase; HSP = heat shock proteins; CM = curcumin; NIR = near-infrared; PEG = Polyethylene Glycol; CuBGM = copper doped Bioactive Glass-ceramic Microspheres.

conducive to bone regeneration is 40–42 °C, and under these conditions new bone and osteoid are at their most abundant [13]. Chen et al. observed that when the osteogenesis temperature of hyperthermia was controlled at about 42 °C, osteogenesis activity was the highest [46].

In addition to the treatment of bone defects, according to Fig. 3, it could be seen that PTT is very advantageous in curing bone defects related to tumours and bone infections, as anti-tumour and antibacterial models were established in many included studies. The therapeutic mechanisms of PTT in tumour and infection are summarized in this systematic review.

Bone metastasis is common in malignant tumours [51], and NIR light-assisted PTT has shown great potential in improving tumour treatment effects and minimising side effects in recent years [52,53]. Tumour cells are sensitive to the temperatures above 41 °C, which accelerate their apoptosis [54]. According to previous reports, the metabolic function of tumour cells may be destroyed or halted at temperatures between 41 °C and 45 °C [48]; irreversible damage will be caused to cancer cells when exposed to environmental temperatures above 48 °C; and tumour cell membranes will collapse, irreversible protein denaturation will occur at temperatures above 50℃ [55]. Many researchers have shown that with photothermal particles, NIR radiation can raise the local temperature to 42–50 °C, thereby promoting tumour hyperthermia ablation [56]. In addition, controlled drug delivery systems mediated by PTT can enhance the killing of any residual tumour cells [52,57]. Yang et al. fabricated multifunctional magnetic mesoporous $SrFe_{12}O_{19}/CaSiO_3$/chitosan scaffolds and, due to the mesopores in the $CaSiO_3$ microspheres, it exhibited great drug delivery properties. Loaded with antitumour drug doxorubicin (DOX), and with the help of static magnetic fields to promote osteogenic differentiation, the scaffolds exerted robust anti-tumour and bone regeneration properties [29].

It is well known that bacterial infection can hinder the osseointegration on the implant surface, and PTT performed by NIR light has attracted many researchers due to its potential antibacterial properties. NIR light-induced hyperthermia counteracts bacteria through various thermal effects, such as the destruction of bacterial integrity or biofilm structure, or denaturation of proteins/enzymes [58]. However, the main problem to be overcome is that the antibacterial effect can only reach >90% efficacy under conditions of around 85 °C, and this excessively high temperature can damage natural tissues and cause other diseases [59,60]. Many studies have confirmed that reactive oxygen species (ROS) such as $^1O_2$ produced by photodynamic therapy (PDT) could kill bacteria by destroying their protein or DNA [61–63]. Huang et al. pointed out that, under the synergistic effect of PTT and PDT produced by a 808 nm laser, the biofilm can be eradicated *in vivo* at the lower temperature of 50 °C [36].

However, it is worth mentioning that although PDT and PTT both belong to the concept of phototherapy, PDT is usually used to kill cells by generating ROS, while PTT can also affect cell proliferation and differentiation through temperature regulation, as described in this paper, promoting osteogenic differentiation of cells. By consulting literatures [64–67], more about the differences between PDT and PTT are summarised in Table 4.

4.2. Polymers used in PTT

In the summarised articles of this systematic review, the mainly used natural polymers were chitosan, alginate and gelatine. The structure of chitosan is similar to glycosaminoglycans (GAG) found in natural tissues, thus it's usually used as a biomimetic biomaterial [68]. The free amino groups of chitosan can be functionalised by carbodiimide chemistry; thus, chitosan can be made into various novel biomaterials for tissue engineering applications [69]. Alginate is a polysaccharide block copolymer with low toxicity, ease of chemical modification, and relatively low cost [68,70]. Alginate scaffolds have the advantage of releasing soluble factors in a required temporal and spatial manner [71], gelatine is a thermo-responsive natural polymer, extracted from collagen. It is biocompatible, non-immunogenic and biodegradable [72]. Recent efforts have focused on the modification of gelatine to manufacture gelatine carriers with different properties for BTE and drug delivery applications. In particular, after being modified by the photo-cross-linkable group, methacrylic acid gelatine (GelMA) has been extensively used in bone repair due to its water-rich features, outstanding cytocompatibility and biodegradability [73]. Yin et al. proved that GelMA hydrogels significantly enhance osteogenic differentiation of stem cells because they possess an intrinsic arginine-glycine-aspartic acid (RGD) sequence [44].

On the other hand, many different types of synthetic polymers were used in the included articles, such as Polylactic acid (PLA), Poly(lactic-co-glycolic) acid (PLGA), Poly(ε-caprolactone) (PCL), Poly(ethylene oxide) (PEG), Poly(vinyl alcohol) (PVA), Polyether ether ketone (PEEK) and Polydopamine (PDA). PLA is a biocompatible, biodegradable aliphatic polyester with high mechanical strength. In addition, PLA has some other forms, such as poly-L-lactide (PLLA) and poly-D-lactide (PDLA), which have different biodegradation rates related to different crystallinity [74]. PLGA is a cyclic dimer copolymerisation of glycolic acid and lactic acid. Due to its biocompatibility, biodegradability, and adjustable mechanical properties, PLGA has been widely used in BTE and drug delivery applications [75]. PCL is a biodegradable polyester, the degradation of PCL *in vivo* is caused by the hydrolysis of ester bonds, resulting in harmless products such as carbon dioxide and water [76,77]. Used as scaffolds in BTE, PCL could maintain high robustness during the healing process owing to its relatively low degradation rate [78]. PEG is a synthetic hydrophilic polymer that has a wide range of biomedical applications due to its low toxicity and biocompatibility [79]. Moreover, with high water content and appropriate mechanical properties, PEG hydrogels could provide suitable microenvironments for cells [80]. PVA possesses appropriate biocompatibility and mechanical properties [81]. The obtained PVA gel is usually not biodegradable under physiological conditions, therefore, it has been used as a permanent scaffold with long-term stability. PEEK has excellent properties such as environmental resistance, non-toxicity, and biocompatibility [82]. The

Table 4
The comparison between PTT and PDT.

	Light source	Mechanism	Common media	Application	Time accuracy
PTT	Light usually in the near-infrared region	Absorb light energy and undergo electronic transitions to convert light energy into heat energy to act on cells	Photothermal agent (PTA): gold nanostructures, carbon-based nanomaterials, black phosphorus and red phosphorus, organic NIR dyes, etc.	Achieve different temperatures to act on cell proliferation and differentiation	The heat continues to diffuse into the surrounding region when the light is switched off
PDT	Diode lasers, light-emitting diode (LED) and filtered lamps, depending on the application	Produce reactive oxygen species (ROS), known as singlet oxygen, to cause cytotoxicity	Photosensitizer (PS): Acridine Orange (AO), Aminolevulinic Acid (ALA), Indocyanine Green (ICG), Methylene Blue (MB), etc.	Kill tumour cells and bacteria with ROS	The immediate chemical changes in PDT cease essentially as soon as the light is switched off

Young's modulus of PEEK is closer to that of human cortical bone, thereby reducing the risk of osteonecrosis and osteoporosis caused by stress shielding [83,84]. PDA is an insoluble biopolymer inspired by mussels, obtained by the polymerisation of its dopamine monomers [85]. PDA has good adhesion property and biocompatibility and can be formed and attached to the surface of almost all materials; this provides a basis for its application in surface functionalisation [86,87]. According to the included literatures, PDA was mostly used to make surface modification coatings for scaffolds and implants.

It is worth noting that due to the weak attachment of cells to synthetic polymers, synthetic polymers are usually used in combination with natural ones to obtain satisfactory characteristics [28]. Yin et al. developed a novel multifunctional implant (SP@MX/GelMA) that consisted of MXene nanosheets, GelMA hydrogels, and sulfonated polyetheretherketone. Loading with tobramycin, this implant displayed robust antibacterial properties and superior osteogenesis-promoting capability [44]. In the study of Chen et al., a PLLA nanofiber network with incorporated sodium alginate microspheres, strontium, ibuprofen, and black phosphorus was developed, and it showed improved hydrophilicity, osteoinductivity and excellent NIR-responsive drug release capacity [46].

4.3. The application forms of polymers that function in PTT

In the studies of Wang et al. and Tong et al., synthetic polymer PLGA was prepared into membranes and microspheres through traditional methods, such as the solvent evaporation method. These materials showed good biological properties but were very limited in terms of mechanical strength and shape maintenance [34,13]. Over the past few years, 3D biomaterials have received widespread attention because their interconnected pores could provide space for cell activity, tissue growth, and nutrient transport [88]. In addition, 3D printing technology promoted the application of porous scaffolds by manufacturing customised scaffolds with precise geometry, porosity, composition, and mechanical properties. By manufacturing scaffolds according to specific anatomical geometry, the scaffolds with structures that match the bone defects of individual patients make the precise and personalised treatment possible [89,90]. Moreover, a highly interconnected scaffold can improve osteoconductivity and enable bone cells to adhere to, proliferate from and form extracellular matrices on it [91]. Therefore, 3D printing is an ideal method for preparing scaffolds. According to the included study, Yang et al. designed a $SrCuSi_4O_{10}$/PCL scaffold through 3D printing, this composite scaffold could not only trigger the ablation of osteosarcoma through hyperthermia, but also promoted the regeneration of vascularised bone [40].

As for the antibacterial and osseointegration effects on the surface of implants, surface modification is usually achieved by preparing bioactive coatings [92]. To date, extensive attempts have been made to prepare multifunctional coatings to simultaneously antibacterial and strengthen osseointegration. General surface modification strategies for antibacterial include adding components which resist bacterial adhesion through electrostatic repulsion and super hydrophobicity [35]. It is worth mentioning that, due to the ideal adhesion properties of PDA, compounds that are not directly used as bioactive coatings or grafts can be adsorbed or connected to PDA to achieve "secondary modification" [93]. In the study of Yuan et al. a biocompatible MoS_2/PDA-RGD coating was prepared on a titanium (Ti) implant, this coating enhanced the osteogenic differentiation of mesenchymal stem cells (MSCs) and exhibited effective antibacterial ability when exposed to NIR radiation [37].

In addition, injectable hydrogels possess unique advantages, they can replace implant surgery with minimally invasive injection methods and could form desired shapes to fill irregular defects [94]. The composition of the injectable hydrogel must be similar to the composition of the bone tissue to increase the osteogenic potential. Xu et al. proposed an injectable sodium alginate hydrogel composite doped with Cu_2O and PDA-coated TiO_2 nanoparticles, used it to guide tissue regeneration (GTR). And through dual light regulation (blue and NIR), this hydrogel could switch between antibacterial and osteogenesis modes [45].

4.4. NIR light-responsive photothermal agents in PTT

Traditional PTAs mainly include gold nanostructures, copper-based nanomaterials, graphene oxide and other carbon-based nanomaterials, NIR dyes, black phosphorus and red phosphorus nanosheets [16–19,95]. All these agents show good NIR absorption performance.

Interestingly, due to structure similar to natural eumelanin, PDA can provide a high photothermal conversion efficiency (40%), which is an essential feature for PTT. It shows strong absorption of the NIR light in the region of 700–1100 nm, and can effectively convert the light energy into heat. In a study of Sun et al., they used PDA coating to functionalise curcumin-loaded chitosan nanoparticles and confirmed that PDA has strong NIR light absorption properties, which could treat cancer and promote bone regeneration through PTT [47]. Additionally, Luo et al. designed an injectable hydrogel containing cisplatin (DDP) and PDA-modified nano-hydroxyapatite by oxidising the Schiff base reaction between sodium alginate and chitosan. In view of the strong absorption of PDA in the NIR region, when exposed to an NIR laser, the hydrogel exhibited an excellent photothermal effect [42].

Recently, biodegradable metals (BMs) have gradually become a hot spot in the field of BTE biomaterials due to their good biocompatibility, degradability, and appropriate mechanical properties. It is expected that the BMs will gradually corrode *in vivo* and the released corrosion products will trigger an appropriate host response; then the BMs will completely dissolve after helping the tissue to heal [96]. Our previous studies showed that magnesiun (Mg) particles and zinc (Zn) particles exhibited excellent osteogenic activity [97,98]. Besides, Long et al. confirmed that micro-sized Mg particles could also be used as a photothermal agent for NIR light-mediated PPT [41]. In general, it can be concluded that if BMs particles can be developed as PTAs, they will exert their biological functions and photothermal conversion functions at the same time, which will be a promising choice for tissue engineering and PTT applications.

Besides, numerous studies have focused on developing PTAs with multifunction. Zhou at al. used ferrite ($MnFe_2O_4$) nanoparticles (NPs) made up of iron oxide and manganese oxide NPs as PTA in their study, and confirmed that this material displayed a favourable photothermal conversion property as well as magnetic resonance (MR) imaging property, thus could also be used as a contrast agent for MR imaging to detect tumour [99]. Mao at al. developed a type of Ag/Ag@AgCl/ZnO hybrid nanostructures, in addition to exerting the photothermal effect, the presence of Ag could enhance the antimicrobial activity [100]. Similarly, Liu et al. constructed a CuS/Cur hybrid with photoacoustic responsiveness, in which CuS showed good photothermal and photodynamic effect, and curcumin (Cur), as a kind of herbal medicine, possessed rapid and highly effective bacteria-killing efficacy [101]. Su et al. prepared an oxygen-deficient S-doped TiO_2 layer with enhanced sonocatalytic-photothermal properties, TiO_2 nanoparticles were used as a sonosensitizer which could produce ROS and thus synergized with PTT to improve the antibacterial efficiency [102].

4.5. NIR-II as a new attempt in PTT

According to the summary of this system review, all but one of the studies used NIR light with a wavelength of 808 nm [40], which is regarded as the NIR-I window (650–1000 nm). However, some

scholars pointed out there are inherent limitations of the NIR-I window, such as limited laser penetration (≈1–2 cm) and high tissue scattering. The NIR-II window (1000–1300 nm) with deeper light transmittance (>2 cm) and higher up limit of radiation is more attractive for biomedical applications [40,103]. Therefore, it is imperative to develop NIR-II PTAs for functionalised bone scaffolds to treat bone defects. Yang et al. successfully manufactured a dual-function platform based on the 3D printed Wesselsite [$SrCuSi_4O_{10}$]/PCL composite scaffold, to simultaneously induce osteosarcoma ablation and enhance vascularised bone regeneration through NIR-II light (1064 nm). The high photothermal conversion efficiency of $SrCuSi_4O_{10}$ nanosheets in the NIR-II region gave the scaffold an excellent PTT curative effect on deep osteosarcomas, without any significant side effects [40]. Li et al. proposed CuS nanoparticles modified with cetuximab (Ab), which inhibited the formation of blood vessels and further inhibited cancer cell growth. These nanoparticles had a maximum absorbance at 1065 nm, in the range of the NIR-II window [104]. Previous studies showed that Au nanomaterials, metal sulphur oxides such as Ag_2S and MoO_2, two-dimensional nanomaterials such as niobium carbide (MXene) and semiconductor polymer nanoparticles SPN_1, SPN_2 and SPN_3 can be applied as NIR-II absorption materials in PTT [103]. Moreover, Zhu et al. indicated that some NIR-II molecular dyes could be used for cancer imaging and surgery, such as cyanine and Donor-acceptor–donor (D-A-D) structures [105].

4.6. Summary and outlook

Overall, PTT is a minimally invasive and highly effective method for the treatment of bone defects, and it is also used to treat bone defects associated with tumours and infections. According to the summary of this systematic review, mild local heating can promote cell proliferation and bone regeneration; moderate heat causes negligible damage to normal tissue cells for a short time, but can be fatal to tumour cells; for the healing of infected wounds, hyperthermia (>50 °C) can effectively inhibit bacterial proliferation. However, research on the metabolism and biocompatibility of different PTAs is needed. And in order to ensure the feasibility of clinical application, monitoring of local immune responses and surrounding normal tissue conditions are also required. In addition, the safety and efficacy of this therapy need to be explored in detail according to the actual situation of each individual.

5. Conclusion

The combined application of BTE polymer materials and NIR-assisted PTT could play a positive role in the treatment of bone-related diseases. Polymers could work as tissue supports and delivery vehicles of PTAs, and they could be made into different forms such as 3D scaffolds, injectable hydrogels and coatings. In addition, PTT provides a precise method for the treatment of bone defects with few side effects. Overall, the joint application of BTE polymers and PTT has potential in the bone regeneration applications.

6. Authors' contributions

Liu Y. and Xia D. proposed the ideas; Wang S., Wang F., and Zhao X. did the literature search; Wang S. wrote the article; all the authors have critically revised the scientific content of this article and approved the final version.

Declaration of Competing Interest

The authors declare that they have no known competing financial interests or personal relationships that could have appeared to influence the work reported in this paper.

Acknowledgement

This study was supported by the National Natural Science Foundation of China [grant numbers 82170929, 81970908, 51901003 and 81771039] and the Beijing Natural Science Foundation [grant number L212014].

Data availability

All experimental data within the article are available from the corresponding author upon reasonable.

References

[1] S. Wang, R. Li, D. Xia, X. Zhao, Y. Zhu, R. Gu, J. Yoon, Y. Liu, The impact of Zn-doped synthetic polymer materials on bone regeneration: a systematic review, Stem Cell Res. Ther. 12 (1) (2021) 123, https://doi.org/10.1186/s13287-021-02195-y.
[2] D. Tang, R.S. Tare, L.Y. Yang, D.F. Williams, K.L. Ou, R.O. Oreffo, Biofabrication of bone tissue: approaches, challenges and translation for bone regeneration, Biomaterials 83 (2016) 363–382, https://doi.org/10.1016/j.biomaterials.2016.01.024.
[3] D. Liu, W. Nie, D. Li, W. Wang, L. Zheng, J. Zhang, J. Zhang, C. Peng, X. Mo, C. He, 3D printed PCL/SrHA scaffold for enhanced bone regeneration, Chem. Eng. J. 362 (2019) 269–279, https://doi.org/10.1016/j.cej.2019.01.015.
[4] F. Fahimipour, M. Rasoulianboroujeni, E. Dashtimoghadam, K. Khoshroo, M. Tahriri, F. Bastami, D. Lobner, L. Tayebi, 3D printed TCP-based scaffold incorporating VEGF-loaded PLGA microspheres for craniofacial tissue engineering, Dent. Mater. 33 (2017) 1205–1216, https://doi.org/10.1016/j.dental.2017.06.016.
[5] Y. Qu, B. Wang, B. Chu, C. Liu, X. Rong, H. Chen, J. Peng, Z. Qian, Injectable and thermosensitive hydrogel and PDLLA electrospun nanofiber membrane composites for guided spinal fusion, ACS Appl. Mater. Interfaces 10 (2018) 4462–4470, https://doi.org/10.1021/acsami.7b17020.
[6] A. Entezari, M.V. Swain, J.J. Gooding, I. Roohani, Q. Li, A modular design strategy to integrate mechanotransduction concepts in scaffold-based bone tissue engineering, Acta Biomater. 118 (2020) 100–112, https://doi.org/10.1016/j.actbio.2020.10.012.
[7] G. Chen, N. Chen, Q. Wang, Fabrication and properties of poly(vinyl alcohol)/b-tricalcium phosphate composite scaffolds via fused deposition modeling for bone tissue engineering, Compos. Sci. Technol. 172 (2019) 17–28, https://doi.org/10.1016/j.compscitech.2019.01.004.
[8] M. Askari, M. Afzali Naniz, M. Kouhi, A. Saberi, A. Zolfagharian, M. Bodaghi, Recent progress in extrusion 3D bioprinting of hydrogel biomaterials for tissue regeneration: a comprehensive review with focus on advanced fabrication techniques, Biomater. Sci. 9 (3) (2021) 535–573, https://doi.org/10.1039/d0bm00973c.
[9] M. Shirzad, A. Zolfagharian, A. Matbouei, M. Bodaghi, Design, evaluation, and optimization of 3D printed truss scaffolds for bone tissue engineering, J. Mech. Behav. Biomed. Mater. 120 (2021) 104594, https://doi.org/10.1016/j.jmbbm.2021.104594.
[10] Y. Yang, J. Aw, B. Xing, Nanostructures for NIR light-controlled therapies, Nanoscale 9 (11) (2017) 3698–3718.
[11] J. Son, G. Yi, J. Yoo, C. Park, H. Koo, H.S. Choi, Light-responsive nanomedicine for biophotonic imaging and targeted therapy, Adv. Drug Deliv. Rev. 138 (2019) 133–147, https://doi.org/10.1016/j.addr.2018.10.002.
[12] W. Zhao, Y. Zhao, Q. Wang, T. Liu, J. Sun, R. Zhang, Remote Light-Responsive Nanocarriers for Controlled Drug Delivery: Advances and Perspectives, Small 15 (2019) e1903060, https://doi.org/10.1002/smll.201903060.
[13] L. Tong, Q. Liao, Y. Zhao, H. Huang, A. Gao, W. Zhang, X. Gao, W. Wei, M. Guan, P.K. Chu, H. Wang, Near-infrared light control of bone regeneration with biodegradable photothermal osteoimplant, Biomaterials 193 (2019) 1–11, https://doi.org/10.1016/j.biomaterials.2018.12.008.
[14] A. Saneja, R. Kumar, D. Arora, S. Kumar, A.K. Panda, S. Jaglan, Recent advances in near-infrared light-responsive nanocarriers for cancer therapy, Drug Discov. Today 23 (2018) 1115–1125, https://doi.org/10.1016/j.drudis.2018.02.005.
[15] R. Weissleder, A clearer vision for in vivo imaging, Nat. Biotechnol. 19 (4) (2001) 316–317, https://doi.org/10.1038/86684.
[16] Y. Ma, X. Liang, S. Tong, G. Bao, Z. Dai, Gold nanoshell nanomicelles for potential magnetic resonance imaging, light-triggered drug release, and photothermal therapy, Adv. Funct. Mater. 23 (7) (2013) 815–822, https://doi.org/10.1002/adfm.201201663.

[17] Y. Li, W. Lu, Q. Huang, C. Li, W. Chen, Copper sulfide nanoparticles for photothermal ablation of tumor cells, Nanomedicine 5 (8) (2010) 1161–1171, https://doi.org/10.2217/nnm.10.85.
[18] W. Zhang, Z. Guo, D. Huang, Z. Liu, X. Guo, H. Zhong, Synergistic effect of chemo-photothermal therapy using PEGylated graphene oxide, Biomaterials 32 (33) (2011) 8555–8561, https://doi.org/10.1016/j.biomaterials.2011.07.071.
[19] B. Yang, J. Yin, Y. Chen, S. Pan, H. Yao, Y. Gao, J. Shi, 2D-black-phosphorus-reinforced 3D-printed scaffolds: A stepwise countermeasure for osteosarcoma 1705611.1–1705611.12, Adv Mater. 30 (10) (2018), https://doi.org/10.1002/adma.201705611.
[20] X. Shi, B. Sitharaman, Q.P. Pham, F. Liang, K. Wu, W.E. Billups, L.J. Wilson, A.G. Mikos, Fabrication of porous ultra-short single-walled carbon nanotube nanocomposite scaffolds for bone tissue engineering, Biomaterials 28 (28) (2007) 4078–4090, https://doi.org/10.1016/j.biomaterials.2007.05.033.
[21] V. Asadian-Ardakani, S. Saber-Samandari, S. Saber-Samandari, The effect of hydroxyapatite in biopolymer-based scaffolds on release of naproxen sodium, J. Biomed. Mater. Res. A 104 (12) (2016) 2992–3003, https://doi.org/10.1002/jbm.a.35838.
[22] W. Pon-On, P. Suntornsaratoon, N. Charoenphandhu, J. Thongbunchoo, N. Krishnamra, I.M. Tang, Hydroxyapatite fromfish scale for potential use as bone scaffold or regenerative material, Mater. Sci. Eng. C Mater. Biol. Appl. 62 (2016) 183–189, https://doi.org/10.1016/j.msec.2016.01.051.
[23] S. Saravanan, D.K. Sameera, A. Moorthi, N. Selvamurugan, Chitosan scaffolds containing chicken feather keratin nanoparticles for bone tissue engineering, Int. J. Biol. Macromol. 62 (2013) 481–486, https://doi.org/10.1016/j.ijbiomac.2013.09.034.
[24] W. Zhao, J. Li, K. Jin, W. Liu, X. Qiu, C. Li, Fabrication of functional PLGA-based electrospun scaffolds and their applications in biomedical engineering, Mater. Sci. Eng. C Mater. Biol. Appl. 59 (2016) 1181–1194, https://doi.org/10.1016/j.msec.2015.11.026.
[25] F. Beladi, S. Saber-Samandari, S. Saber-Samandari, Cellular compatibility of nanocomposite scaffolds based on hydroxyapatite entrapped in cellulose network for bone repair, Mater. Sci. Eng. C Mater. Biol. Appl. 75 (2017) 385–392, https://doi.org/10.1016/j.msec.2017.02.040.
[26] B.S. Kim, I.K. Park, T. Hoshiba, H.L. Jiang, C.S. Cho, Design of artificial extracellular matrices for tissue engineering, Prog. Polym. Sci. 36 (2) (2011) 238–268, https://doi.org/10.1016/j.progpolymsci.2010.10.001.
[27] B.M. Holzapfel, J.C. Reichert, J.T. Schantz, U. Gbureck, L. Rackwitz, U. Nöth, F. Jakob, M. Rudert, J. Groll, D.W. Hutmacher, How smart do biomaterials need to be? A translational science and clinical point of view, Adv. Drug Deliv. Rev. 65 (4) (2013) 581–603, https://doi.org/10.1016/j.addr.2012.07.009.
[28] F. Rosso, G. Marino, A. Giordano, M. Barbarisi, D. Parmeggiani, A. Barbarisi, Smart materials as scaffolds for tissue engineering, J. Cell. Physiol. 203 (3) (2005) 465–470, https://doi.org/10.1002/jcp.20270.
[29] F. Yang, J. Lu, Q. Ke, X. Peng, Y. Guo, X. Xie, Magnetic Mesoporous Calcium Sillicate/Chitosan Porous Scaffolds for Enhanced Bone Regeneration and Photothermal-Chemotherapy of Osteosarcoma, Sci. Rep. 8 (1) (2018) 7345, https://doi.org/10.1038/s41598-018-25595-2.
[30] J.W. Lu, F. Yang, Q.F. Ke, X.T. Xie, Y.P. Guo, Magnetic nanoparticles modified-porous scaffolds for bone regeneration and photothermal therapy against tumors, Nanomedicine 14 (3) (2018) 811–822, https://doi.org/10.1016/j.nano.2017.12.025.
[31] Y. Lu, L. Li, M. Li, Z. Lin, L. Wang, Y. Zhang, Q. Yin, H. Xia, G. Han, Zero-Dimensional Carbon Dots Enhance Bone Regeneration, Osteosarcoma Ablation, and Clinical Bacterial Eradication, Bioconjug. Chem. 29 (9) (2018) 2982–2993, https://doi.org/10.1021/acs.bioconjchem.8b00400.
[32] S. Saber-Samandari, M. Mohammadi-Aghdam, S. Saber-Samandari, A novel magnetic bifunctional nanocomposite scaffold for photothermal therapy and tissue engineering, Int. J. Biol. Macromol. 138 (2019) 810–818, https://doi.org/10.1016/j.ijbiomac.2019.07.145.
[33] P. Zhao, Y. Ge, X. Liu, Q. Ke, J. Zhang, Z. Zhu, Y. Guo, Ordered arrangement of hydrated GdPO4 nanorods in magnetic chitosan matrix promotes tumor photothermal therapy and bone regeneration against breast cancer bone metastases, Chem. Eng. J. 381 (2020) 122694, https://doi.org/10.1016/j.cej.2019.122694.
[34] X. Wang, J. Shao, M. Abd El Raouf, H. Xie, H. Huang, H. Wang, P.K. Chu, X.F. Yu, Y. Yang, A.M. AbdEl-Aal, N.H.M. Mekkaway, R.J. Miron, Y. Zhang, Near-infrared light-triggered drug delivery system based on black phosphorus for in vivo bone regeneration, Biomaterials 179 (2018) 164–174, https://doi.org/10.1016/j.biomaterials.2018.06.039.
[35] M. Li, L. Li, K. Su, X. Liu, T. Zhang, Y. Liang, D. Jing, X. Yang, D. Zheng, Z. Cui, Z. Li, S. Zhu, K.W.K. Yeung, Y. Zheng, X. Wang, S. Wu, Highly Effective and Noninvasive Near-Infrared Eradication of a Staphylococcus aureus Biofilm on Implants by a Photoresponsive Coating within 20 Min, Adv. Sci. (Weinh) 6 (17) (2019) 1900599, https://doi.org/10.1002/advs.201900599.
[36] B. Huang, L. Tan, X. Liu, J. Li, S. Wu, A facile fabrication of novel stuff with antibacterial property and osteogenic promotion utilizing red phosphorus and near-infrared light, Bioact. Mater. 4 (1) (2019) 17–21, https://doi.org/10.1016/j.bioactmat.2018.11.002.
[37] Z. Yuan, B. Tao, Y. He, J. Liu, C. Lin, X. Shen, Y. Ding, Y. Yu, C. Mu, P. Liu, K. Cai, Biocompatible MoS(2)/PDA-RGD coating on titanium implant with antibacterial property via intrinsic ROS-independent oxidative stress and NIR irradiation, Biomaterials 217 (2019) 119290, https://doi.org/10.1016/j.biomaterials.2019.119290.
[38] Z. Yuan, B.L. Tao, Y. He, C.Y. Mu, G.H. Liu, J.X. Zhang, Q. Liao, P. Liu, K.Y. Cai, Remote eradication of biofilm on titanium implant via near-infrared light triggered photothermal/photodynamic therapy strategy, Biomaterials 223 (2019) 119479, https://doi.org/10.1016/j.biomaterials.2019.119479.
[39] G. Zhang, X. Zhang, Y. Yang, R. Chi, J. Shi, R. Hang, X. Huang, X. Yao, P.K. Chu, X. Zhang, Dual light-induced in situ antibacterial activities of biocompatibleTiO (2)/MoS(2)/PDA/RGD nanorod arrays on titanium, Biomater. Sci. 8 (1) (2020) 391–404, https://doi.org/10.1039/c9bm01507h.
[40] C. Yang, H. Ma, Z. Wang, M.R. Younis, C. Liu, C. Wu, Y. Luo, P. Huag, 3D Printed Wesselsite Nanosheets Functionalized Scaffold Facilitates NIR-II Photothermal Therapy and Vascularized Bone Regeneration, Adv. Sci. (Weinh) (2021) e2100894, https://doi.org/10.1002/advs.202100894.
[41] J. Long, W. Zhang, Y. Chen, B. Teng, B. Liu, H. Li, Z. Yao, D. Wang, L. Li, X.F. Yu, L. Qin, Y. Lai, Multifunctional magnesium incorporated scaffolds by 3D-Printing for comprehensive postsurgical management of osteosarcoma, Biomaterials 275 (2021) 120950, https://doi.org/10.1016/j.biomaterials.2021. 120950.
[42] S. Luo, J. Wu, Z. Jia, P. Tang, J. Sheng, C. Xie, C. Liu, D. Gan, D. Hu, W. Zheng, X. Lu, An Injectable, Bifunctional Hydrogel with Photothermal Effects for Tumor Therapy and Bone Regeneration, Macromol. Biosci. 19 (9) (2019) e1900047, https://doi.org/10.1002/mabi.201900047.
[43] Y. Li, X. Liu, B. Li, Y. Zheng, Y. Han, D.F. Chen, K.W.K. Yeung, Z. Cui, Y. Liang, Z. Li, S. Zhu, X. Wang, S. Wu, Near-Infrared Light Triggered Phototherapy and Immunotherapy for Elimination of Methicillin-Resistant Staphylococcus aureus Biofilm Infection on Bone Implant, ACS Nano 14 (7) (2020) 8157–8170, https://doi.org/10.1021/acsnano.0c01486.
[44] J. Yin, Q. Han, J. Zhang, Y. Liu, X. Gan, K. Xie, L. Xie, Y. Deng, MXene-Based Hydrogels Endow Polyetheretherketone with Effective Osteogenicity and Combined Treatment of Osteosarcoma and Bacterial Infection, ACS Appl. Mater. Interfaces 12 (41) (2020) 45891–45903, https://doi.org/10.1021/acsami. 0c14752.
[45] Y. Xu, S. Zhao, Z. Weng, W. Zhang, X. Wan, T. Cui, J. Ye, L. Liao, X. Wang, Jelly-Inspired Injectable Guided Tissue Regeneration Strategy with Shape Auto-Matched and Dual-Light-Defined Antibacterial/Osteogenic Pattern Switch Properties, ACS Appl. Mater. Interfaces 12 (49) (2020) 54497–54506, https://doi.org/10.1021/acsami.0c18070.
[46] S. Chen, R. Guo, Q. Liang, X. Xiao, Multifunctional modified polylactic acid nanofibrous scaffold incorporating sodium alginate microspheres decorated with strontium and black phosphorus for bone tissue engineering, J. Biomater. Sci. Polym. Ed. 32 (12) (2021) 1598–1617, https://doi.org/10.1080/09205063.2021.1927497.
[47] X. Sun, Z.Y. Meng, Q.W. Yu, X.Y. Wang, Z. Zhao, Engineering PDA-coated CM-CS nanoparticles for photothermo-chemotherapy of osteosarcoma and bone regeneration, Biochem. Eng. J. 175 (2021), https://doi.org/10.1016/j.bej.2021.108138.
[48] Z. Yang, F.J. Zhao, W. Zhang, Z.Y. Yang, M. Luo, L. Liu, X.D. Cao, D.F. Chen, X.F. Chen, Degradable photothermal bioactive glass composite hydrogel for the sequential treatment of tumor-related bone defects: From anti-tumor to repairing bone defects, Chem. Eng. J. 419 (2021) 129520, https://doi.org/10.1016/j.cej.2021.129520.
[49] S.A. Leon, S.O. Asbell, H.H. Arastu, G. Edelstein, A.J. Packel, S. Sheehan, I. Daskal, G.G. Guttmann, I. Santos, Effects of hyperthermia on bone. II. Heating of bone in vivo and stimulation of bone growth, Int. J. Hyperthermia 9 (1) (1993) 77–87, https://doi.org/10.3109/02656739309061480.
[50] C. Shui, A. Scutt, Mild heat shock induces proliferation, alkaline phosphatase activity, and mineralization in human bone marrow stromal cells and mg-63 cells in vitro, J. Bone Miner. Res. 16 (4) (2001) 731–741, https://doi.org/10.1359/jbmr.2001.16.4.731.
[51] E. Verron, H. Schmid-Antomarchi, H. Pascal-Mousselard, A. Schmid-Alliana, J. C. Scimeca, J.M. Bouler, Therapeutic strategies for treating osteolytic bone metastases, Drug Discov. Today. 19 (9) (2014) 1419–1426, https://doi.org/10.1016/j.drudis.2014.04.004.
[52] A.L. Volsi, C. Scialabba, V. Vetri, G. Cavallaro, M. Licciardi, G. Giammona, Near-Infrared Light Responsive Folate Targeted Gold Nanorods for Combined Photothermal-Chemotherapy of Osteosarcoma, ACS Appl. Mater. Interfaces 9 (16) (2017) 14453–14469, https://doi.org/10.1021/acsami.7b03711.
[53] Z. Li, H. Huang, S. Tang, Y. Li, X.F. Yu, H. Wang, P. Li, Z. Sun, H. Zhang, C. Liu, P. K. Chu, Small gold nanorods laden macrophages for enhanced tumor coverage in photothermal therapy, Biomaterials 74 (2016) 144–154, https://doi.org/10.1016/j.biomaterials.2015.09.038.
[54] H. Wang, X. Zeng, L. Pang, H. Wang, B. Lin, Z. Deng, E.L.X. Qi, N. Miao, D. Wang, P. Huang, H. Hu, J. Li, Integrative treatment of anti-tumor/bone repair by combination of MoS2 nanosheets with 3D printed bioactive borosilicate glass scaffolds, Chem. Eng. J. 396 (2020) 125081, https://doi.org/10.1016/j.cej.2020.125081.
[55] D. Jaque, M.L. Martínez, R.B. Del, P. Harogonzalez, A. Benayas, J.L. Plaza, R.E. Martín, S.J. García, Nanoparticles for Photothermal Therapies, Nanoscale 6 (16) (2014) 9494–9530, https://doi.org/10.1039/c4nr00708e.
[56] J. Kolosnjaj-Tabi, R.D. Corato, L. Lartigue, I. Marangon, P. Guardia, A.K.A. Silva, N. Luciani, O. Clément, P. Flaud, J.V. Singh, P. Decuzzi, T. Pellegrino, C. Wilhelm, F. Gazeau, Heat-generating iron oxide nanocubes: subtle "destructurators" of the tumoral microenvironment, ACS Nano 8 (5) (2014) 4268–4283, https://doi.org/10.1021/nn405356r.
[57] C.F. Adams, M.R. Pickard, D.M. Chari, Magnetic nanoparticle mediated transfection of neural stem cell suspension cultures is enhanced by applied oscillating magnetic fields, Nanomedicine 9 (6) (2013) 737–741, https://doi.org/10.1016/j.nano.2013.05.014.

[58] S.H. Kim, E.B. Kang, C.J. Jeong, S.M. Sharker, I. In, S.Y. Park, Light controllable surface coating for effective photothermal killing of bacteria, ACS Appl. Mater. Interfaces 7 (28) (2015) 15600–15606, https://doi.org/10.1021/acsami.5b04321.
[59] C. He, X. Duan, N. Guo, C. Chan, C. Poon, R.R. Weichselbaum, W. Lin, Core-shell nanoscale coordination polymers combine chemotherapy and photodynamic therapy to potentiate checkpoint blockade cancer immunotherapy, Nat. Commun. 7 (2016) 12499, https://doi.org/10.1038/ncomms12499.
[60] C. Mao, Y. Xiang, X. Liu, Z. Cui, X. Yang, Z. Li, S. Zhu, Y. Zheng, K.W.K. Yeung, S. Wu, Repeatable photodynamic therapy with triggered signaling pathways of fibroblast cell proliferation and differentiation to promote bacteria-accompanied wound healing, ACS Nano 12 (2) (2018) 1747–1759, https://doi.org/10.1021/acsnano.7b08500.
[61] X. Li, D. Lee, J. Huang, J. Yoon, Phthalocyanine-assembled nanodots as photosensitizers for highly efficient type I photoreactions in photodynamic therapy, Angew. Chem. Int. Ed. Engl. 57 (31) (2018) 9885–9890, https://doi.org/10.1002/anie.201806551.
[62] Z. Feng, X. Liu, L. Tan, Z. Cui, X. Yang, Z. Li, Y. Zheng, K.W.K. Yeung, S. Wu, Electrophoretic deposited stable chitosan@MoS2 coating with rapid in Situ bacteria-killing ability under dual-light irradiation, Small 14 (21) (2018) e1704347, https://doi.org/10.1002/smll.201704347.
[63] M. Li, X. Liu, L. Tan, Z. Cui, X. Yang, Z. Li, Y. Zheng, K.W.K. Yeung, P.K. Chu, S. Wu, Noninvasive rapid bacteria-killing and acceleration of wound healing through photothermal/photodynamic/copper ion synergistic action of a hybrid hydrogel, Biomater. Sci. 6 (8) (2018) 2110–2121, https://doi.org/10.1039/c8bm00499d.
[64] J. Sun, F. Xing, J. Braun, F. Traub, P.M. Rommens, Z. Xiang, et al., Progress of Phototherapy Applications in the Treatment of Bone Cancer, Int. J. Mol. Sci. 22 (21) (2021) 11354, https://doi.org/10.3390/ijms222111354.
[65] B.C. Wilson, R.A. Weersink, The Yin and Yang of PDT and PTT, Photochem. Photobiol. 96 (2) (2020) 219–231, https://doi.org/10.1111/php.13184.
[66] W. Bu, Y. Wang, X. Chen, F. Fang, Novel strategy in giant cutaneous squamous cell carcinoma treatment: The case experience with a combination of photodynamic therapy and surgery, Photodiagnosis Photodyn. Ther. 19 (2017) 116–118, https://doi.org/10.1016/j.pdpdt.2017.05.006.
[67] M. Zhou, Y. Xing, X. Li, X. Du, T. Xu, X. Zhang, Cancer Cell Membrane Camouflaged Semi-Yolk@Spiky-Shell Nanomotor for Enhanced Cell Adhesion and Synergistic Therapy, Small 16 (39) (2020) e2003834, https://doi.org/10.1002/smll.202003834.
[68] M. Izydorczyk, S.W. Cui, Q. Wang, Polysaccharide gums: Structures, functional properties, and applications, in: Food Carbohydrates: Chemistry, Physical Properties, and Applications, CRC Press, 2005, pp. 263–307.
[69] I.K. Park, J. Yang, H.J. Jeong, H.S. Bom, I. Harada, T. Akaike, S.I. Kim, C.S. Cho, Galactosylated chitosan as a synthetic extracellular matrix for hepatocytes attachment, Biomaterials 24 (13) (2003) 2331–2337, https://doi.org/10.1016/s0142-9612(03)00108-x.
[70] J.A. Rowley, G. Madlambayan, D.J. Mooney, Alginate hydrogels as synthetic extracellular matrix materials, Biomaterials 20 (1) (1999) 45–53, https://doi.org/10.1016/s0142-9612(98)00107-0.
[71] J. Sun, H. Tan, Alginate-based biomaterials for regenerative medicine applications, Materials (Basel) 6 (4) (2013) 1285–1309, https://doi.org/10.3390/ma6041285.
[72] Y. Tabata, Biomaterial technology for tissue engineering applications, J. R. Soc. Interface 6 (Suppl 3) (2009) S311–S324, https://doi.org/10.1098/rsif.2008.0448.focus.
[73] K. Yue, G. Trujillo-de Santiago, M.M. Alvarez, A. Tamayol, N. Annabi, A. Khademhosseini, Synthesis, Properties, and Biomedical Applications of Gelatin Methacryloyl (GelMA) Hydrogels, Biomaterials 73 (2015) 254–271, https://doi.org/10.1016/j.biomaterials.2015.08.045.
[74] C. Chung, J.A. Burdick, Engineering cartilage tissue, Adv. Drug Deliv. Rev. 60 (2) (2008) 243–262, https://doi.org/10.1016/j.addr.2007.08.027.
[75] H.K. Makadia, S.J. Siegel, Poly lactic-co-glycolic acid (PLGA) as biodegradable controlled drug delivery carrier, Polymers (Basel) 3 (3) (2011) 1377–1397, https://doi.org/10.3390/polym3031377.
[76] I. Engelberg, J. Kohn, Physico-mechanical properties of degradable polymers used in medical applications: A comparative study, Biomaterials 12 (3) (1991) 292–304, https://doi.org/10.1016/0142-9612(91)90037-b.
[77] P.A. Gunatillake, R. Adhikari, Biodegradable synthetic polymers for tissue engineering, Eur. Cell. Mater. 5 (1–16) (2003), https://doi.org/10.22203/ecm.v005a01. discussion 16.
[78] J. Hao, M. Yuan, X. Deng, Biodegradable and biocompatible nanocomposites of poly(ε-caprolactone) with hydroxyapatite nanocrystals: Thermal and mechanical properties, J. Appl. Polym. Sci. 86 (3) (2010) 676–683, https://doi.org/10.1002/app.10955.
[79] J.M. Harris, Introduction to biotechnical and biomedical applications of poly (ethylene glycol), Springer, New York, 1992, pp. 11–14.
[80] A. Bharadwaz, A.C. Jayasuriya, Recent trends in the application of widely used natural and synthetic polymer nanocomposites in bone tissue regeneration, Mater. Sci. Eng. C Mater. Biol. Appl. 110 (2020) 110698, https://doi.org/10.1016/j.msec.2020.110698.
[81] S. Shafiei, M. Omidi, F. Nasehi, H. Golzar, D. Mohammadrezaei, M.R. Rad, A. Khojasteh, Egg shell-derived calcium phosphate/carbon dot nanofibrous scaffolds for bone tissue engineering: Fabrication and characterization, Mater. Sci. Eng. C Mater. Biol. Appl. 100 (2019) 564–575, https://doi.org/10.1016/j.msec.2019.03.003.
[82] S. Bose, D. Ke, H. Sahasrabudhe, A. Bandyopadhyay, Additive Manufacturing of Biomaterials, Prog. Mater. Sci. 93 (2018) 45–111, https://doi.org/10.1016/j.pmatsci.2017.08.003.
[83] L. Wang, S. He, X. Wu, S. Liang, Z. Mu, J. Wei, F. Deng, Y. Deng, S. Wei, Polyetheretherketone/Nano-Fluorohydroxyapatite Composite With Antimicrobial Activity and Osseointegration Properties, Biomaterials 35 (25) (2014) 6758–16575, https://doi.org/10.1016/j.biomaterials.2014.04.085.
[84] F.B. Torstrick, A.S.P. Lin, D. Potter, D.L. Safranski, T.A. Sulchek, K. Gall, R.E. Guldberg, Porous PEEK Improves the Bone-Implant Interface Compared to Plasma-Sprayed Titanium Coating on PEEK, Biomaterials 185 (2018) 106–116, https://doi.org/10.1016/j.biomaterials.2018.09.009.
[85] H. Lee, S.M. Dellatore, W.M. Miller, P.B. Messersmith, Mussel-inspired surface chemistry for multifunctional coatings, Science 318 (5849) (2007) 426–430, https://doi.org/10.1126/science.1147241.
[86] G.S.R. Raju, L. Benton, E. Pavitra, J.S. Yu, Multifunctional nanoparticles: recent progress in cancer therapeutics, Chem. Commun. (Camb.) 51 (68) (2015) 13248–13259, https://doi.org/10.1039/c5cc04643b.
[87] M.J. Harrington, A. Masic, N. Holten-Andersen, J.H. Waite, P. Fratzl, Iron-clad fibers: a metal-based biological strategy for hard flexible coatings, Science 328 (5975) (2010) 216–220, https://doi.org/10.1126/science.1181044.
[88] B. Derby, Printing and prototyping of tissues and scaffolds, Science 338 (6109) (2012) 921–926, https://doi.org/10.1126/science.1226340.
[89] L. Zhang, G. Yang, B.N. Johnson, X. Jia, Three-dimensional (3D) printed scaffold and material selection for bone repair, Acta Biomater. 84 (2019) 16–33, https://doi.org/10.1016/j.actbio.2018.11.039.
[90] S.V. Murphy, A. Atala, 3D bioprinting of tissues and organs, Nat. Biotechnol. 32 (8) (2014) 773–785, https://doi.org/10.1038/nbt.2958.
[91] V. Karageorgiou, D. Kaplan, Porosity of 3D biomaterial scaffolds and osteogenesis, Biomaterials 26 (27) (2005) 5474–5491, https://doi.org/10.1016/j.biomaterials.2005.02.002.
[92] L. Zhang, C. Ning, T. Zhou, X. Liu, K.W.K. Yeung, T. Zhang, Z. Xu, X. Wang, S. Wu, P.K. Chu, Polymeric nanoarchitectures on Ti-based implants for antibacterial applications, ACS Appl. Mater. Interfaces 6 (20) (2014) 17323–17345, https://doi.org/10.1021/am5045604.
[93] A. Jin, Y. Wang, K. Lin, L. Jiang, Nanoparticles modified by polydopamine: Working as "drug" carriers, Bioact. Mater. 5 (3) (2020) 522–541, https://doi.org/10.1016/j.bioactmat.2020.04.003.
[94] K. Ren, C. He, C. Xiao, G. Li, X. Chen, Injectable glycopolypeptide hydrogels as biomimetic scaffolds for cartilage tissue engineering, Biomaterials 51 (2015) 238–249, https://doi.org/10.1016/j.biomaterials. 2015.02.026.
[95] A. Yuan, X. Qiu, X. Tang, W. Liu, J. Wu, Y. Hu, Self-assembled PEG-IR-780-C13 micelle as a targeting, safe and highly-effective photothermal agent for in vivo imaging and cancer therapy, Biomaterials 51 (2015) 184–193, https://doi.org/10.1016/j.biomaterials.2015.01.069.
[96] Y. Zheng, X. Gu, F. Witte, Biodegradable metals, Mater. Sci. Eng. R Rep. 77 (2014) 1–34, https://doi.org/10.1016/j.mser.2014.01.001.
[97] F. Wang, X. Xia, S. Wang, R. Gu, F. Yang, X. Zhao, et al., Photocrosslinkable Col/PCL/Mg composite membrane providing spatiotemporal maintenance and positive osteogenetic effects during guided bone regeneration, Bioact. Mater. 13 (2022) 53–63, https://doi.org/10.1016/j.bioactmat.2021.10.019.
[98] S. Wang, R. Gu, F. Wang, X. Zhao, F. Yang, Y. Xu, et al., 3D-Printed PCL/Zn scaffolds for bone regeneration with a dose-dependent effect on osteogenesis and osteoclastogenesis, Mater. Today Bio. 13 (2022) 100202, https://doi.org/10.1016/j.mtbio.2021.100202.
[99] B. Zhou, Q. Wu, M. Wang, A. Hoover, X. Wang, F. Zhou, et al., Immunologically modified MnFe(2)O(4) nanoparticles to synergize photothermal therapy and immunotherapy for cancer treatment, Chem. Eng. J. 396 (2020) 125239, https://doi.org/10.1016/j.cej.2020.125239.
[100] C. Mao, Y. Xiang, X. Liu, Z. Cui, X. Yang, K.W.K. Yeung, et al., Photo-Inspired Antibacterial Activity and Wound Healing Acceleration by Hydrogel Embedded with Ag/Ag@AgCl/ZnO Nanostructures, ACS Nano 11 (9) (2017) 9010–9021, https://doi.org/10.1021/acsnano.7b03513.
[101] H. Liu, J. Li, X. Liu, Z. Li, Y.u. Zhang, Y. Liang, Y. Zheng, S. Zhu, Z. Cui, S. Wu, Photo-Sono Interfacial Engineering Exciting the Intrinsic Property of Herbal Nanomedicine for Rapid Broad-Spectrum Bacteria Killing, ACS Nano 15 (11) (2021) 18505–18519.
[102] K. Su, L. Tan, X. Liu, Z. Cui, Y. Zheng, B. Li, et al., Rapid Photo-Sonotherapy for Clinical Treatment of Bacterial Infected Bone Implants by Creating Oxygen Deficiency Using Sulfur Doping, ACS Nano 14 (2) (2020) 2077–2089, https://doi.org/10.1021/acsnano.9b08686.
[103] Y. Zhang, S. Zhang, Z. Zhang, L. Ji, J. Zhang, Q. Wang, T. Guo, S. Ni, R. Cai, X. Mu, W. Long, H. Wang, Recent Progress on NIR-II Photothermal Therapy, Front. Chem. 9 (2021) 728066, https://doi.org/10.3389/fchem.2021.728066.
[104] B. Li, Z. Jiang, D. Xie, Y. Wang, X. Lao, Cetuximab-modified CuS nanoparticles integrating near-infrared-II-responsive photothermal therapy and anti-vessel treatment, Int. J. Nanomed. 8 (13) (2018) 7289–7302, https://doi.org/10.2147/IJN.S175334.
[105] S. Zhu, R. Tian, A.L. Antaris, X. Chen, H. Dai, Near-infrared-II molecular dyes for cancer imaging and surgery, Adv. Mater. 31 (24) (2019) e1900321, https://doi.org/10.1002/adma.201900321.